Journal Name

Crossmark

RECEIVED
dd Month yyyy

REVISED
dd Month yyyy

PAPER

Infinite Blueshift as a Challenge to Past Eternal Inflation

Jonathan Gratus[1,2,*] and Sam Close[3]

[1]Department of Physics, Lancaster University, Lancaster, UK
[2]The Cockcroft Institute, Daresbury, UK
[3]School of Mathematical Sciences, University of Nottingham, Nottingham, UK
[*]Author to whom any correspondence should be addressed.

E-mail: j.gratus@lancaster.ac.uk

Keywords: cosmology, eternal inflation, de Sitter space

Abstract

An observer in an eternally inflating universe, also known as a de Sitter universe, will see distant objects rushing towards them, in that both the distant objects' angular sizes will increase and light from these objects will be unboundedly blueshifted. They will produce a flash of infinite intensity when they first appear. The inflationary coordinate system contains a coordinate singularity and the light is emitted on the other side of this coordinate singularity. Our results are applicable to all universes which have eternal inflation in the past, whatever their current state. For a universe with a finite number of e-folds of inflation, we use this analysis to give an upper limit on the number of e-folds of the order of around 100.

1 Introduction

The modern consensus in cosmology is that the early universe underwent a period of rapid expansion, in a process called inflation [1, 2, 3]. Inflation is deemed necessary to explain some of the observations that the naïve hot big-bang model cannot: in particular, it tackles the horizon problem, monopole problem, and flatness problem, amongst others.

In this article we consider what we, as observers in an eternally inflating universe, would actually observe. We primarily concern ourselves with *universes which had eternal inflation in the past*, whether or not the present and future universe is inflating. This is particularly relevant in the study of bubble universes (see [4, 5, 6] for a non-exhaustive list of recent examples). For this paper we assume that gravitational sources in our universe are weak on a cosmological scale, and thus only provide a perturbation to metric. In particular, they do not change the geometry of the spacetime.

The Penrose diagram for de Sitter space is well known [7], however, in this article, Section 3, we look at what would be observed by an observer in such a past infinite de Sitter space. To the best of the authors' knowledge, these results have not previously stated in the literature.

Objects close to us would behave as expected, accelerating away, until they cross the cosmological horizon. Counter-intuitively, more distant objects will actually be observed rushing towards us, understood as their angular size in the sky increasing. Since everything is rushing towards us, most objects would be blueshifted, with the blueshift increasing unboundedly with distance. To avoid this blueshift, the source object has to be initially travelling asymptotically at the speed of light away from us.

The reason we do not normally consider such distant "stars" is that the standard metric for inflation contains a coordinate singularity $\mathcal{H}^\infty$, and the observation of these blueshifted stars requires that they emit their light on the other side of this coordinate singularity. By "stars", we mean any light producing source, not necessarily a stellar object. This coordinate singularity is not obvious as it involves a limit as time goes to the infinite past. de Sitter space possesses a *global coordinate system* which is well-behaved at $\mathcal{H}^\infty$ and does not have the coordinate singularity. This is depicted as the red and blue lines in Figure 1. Here we can see that the standard comoving coordinate system does not cover de Sitter space, and that there is the coordinate singularity $\mathcal{H}^\infty$.

We, as observers, can now distinguish two types of worldlines. Those, like the red lines in Figure 1, we call *initially coincident worldlines* (ICW). These are the only ones considered in the inflationary model. The other worldlines we call *Copernican* worldlines. This reflects the

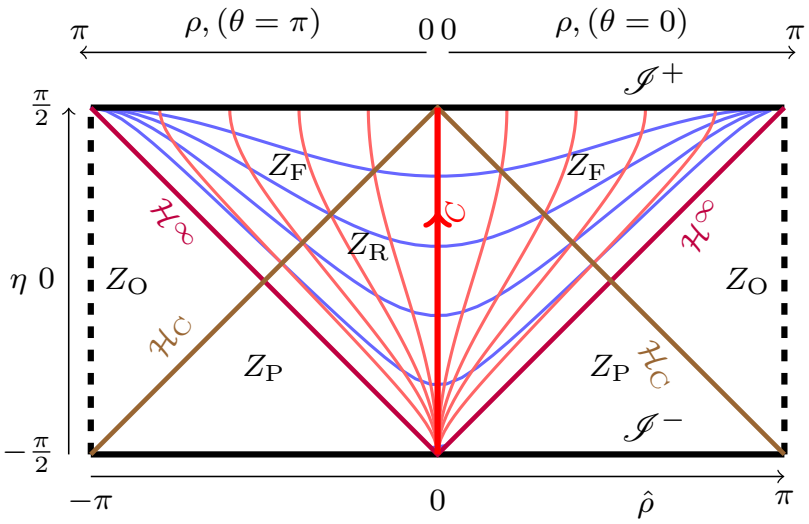

Figure 1. The annulus A, unwrapped in $(\eta, \hat{\rho})$ coordinates. The bottom line, $\eta = -\pi/2$ is the past boundary $\mathscr{I}^-$, while the upper line $\eta = \pi/2$ is the future boundary $\mathscr{I}^+$. The left-hand dashed boundary $\hat{\rho} = -\pi$ is identified with the right-hand dashed boundary $\hat{\rho} = \pi$. Above the figure, the coordinate $0 < \rho < \pi$, is given. The thick red line is the worldline C, which partitions spacetime into the four zones, $Z_{\rm R}$, $Z_{\rm F}$, $Z_{\rm P}$ and $Z_{\rm O}$. The boundaries of these zones are the lightcones $\mathcal{H}^\infty$ and $\mathcal{H}_C$. The standard comoving coordinates (t, r) (which we refer to as the *inflationary coordinates*) are also depicted. The red curves are worldlines with constant r, and the blue curves are hypersurfaces of constant t.

assumption that there is nothing special about ICWs. It is these worldlines which are infinitely blueshifted.

de Sitter space corresponds to a universe which is eternally inflating in both the past and future with a constant Hubble parameter. Our universe could have eternal inflation in the past, future, both, or neither. Since we are concerned with what an observer would see, our results presented here also apply to any past eternal inflation, even if the current universe is not in an inflationary phase. Thus our results also apply to bubble cosmologies.

The simple observation that the night sky does not contain intensely blueshifted "stars" implies that one of the assumptions in our model is not valid. The simplest counter model, which coincides with the standard inflationary model of our universe, is that the period of inflation did not stretch back to the infinite past. This is in agreement with the Borde-Guth-Vilenkin theorem [8]. Flatness and removal of magnetic monopoles require a minimum of 50-60 e-folds of inflation. By simple calculations, comparing the maximum energy of photons observed and an estimate of the maximum energy photons before inflation, we conclude a maximum of $\mathcal{O}(10^2)$ e-folds of inflation. There are other proposed upper limits on the number of e-folds [9, 10, 11].

This article is structured as follows: in Section 2, we describe for context and completeness the inflationary, global, embedded and radar coordinate systems for de Sitter space and the coordinate transformations between them. In Section 3, we discuss observations one would or could make in an eternally inflating universe. We comment on the fact that Copernican particles would not be able to thermalise. We show how one can apply these results to the case when the universe only has a finite number of e-folds of inflation. We consider the maximum photon energy observed, to derive a maximum number of e-folds. In the conclusion we consider mechanisms which can prevent infinite blueshift. These include limiting the number of e-folds, not having light in the universe, considering all matter initially rushing away from us and the gamma rays being consumed by black holes. We also consider different directions of future research.

2 Global coordinate systems and the Penrose diagram

The standard metric for inflation, with $c = G = 1$ and signature $(-,+,+,+)$, is given by the standard comoving coordinate system (which we refer to as the *inflationary coordinate system*) (t, r, θ, ϕ)

$$-\infty < t < \infty, \quad 0 < r < \infty, \quad 0 < \theta < \pi \quad \text{and} \quad 0 < \phi < 2\pi. \tag{1}$$

This is given by

$$\mathrm{d}s^2 = -\,\mathrm{d}t^2 + e^{2\Lambda t}(\mathrm{d}r^2 + r^2\,\mathrm{d}\omega^2) \tag{2}$$

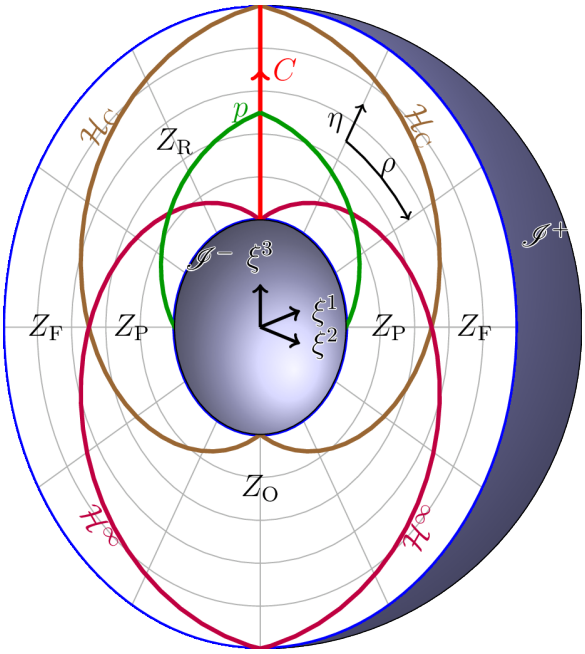

Figure 2. 1+2–dimensional version of de Sitter space M_3, in the (ξ^1, ξ^2, ξ^3) coordinate system. It consists of a hollow ball $\pi/2 < R < 3\pi/2$ where $R^2 = (\xi^1)^2 + (\xi^2)^2 + (\xi^3)^2$. The inner sphere is $\mathscr{I}^-$ and is the initial point of all worldlines, while the outer sphere is $\mathscr{I}^+$ and is the final point.
We have sliced through M_3, with $\xi^1 = 0$, to depict the thick hemisphere with $\xi^1 \geq 0$, with the slice being the annulus A. The red line represents an observer C at rest. The boundary causal future of C is the brown curve $\mathcal{H}_C$, while the boundary of the causal past is the purple curve $\mathcal{H}^\infty$. These are rotated about the vertical axis. The curves $\mathcal{H}_C$ and $\mathcal{H}^\infty$ partition M_3 into four zones, Z_R, Z_F, Z_P and Z_O. The point p is an event on C and the green lines are the boundary of its past lightcone.

where Λ is the cosmological constant and the spherical metric is given by

$$\mathrm{d}\omega^2 = \mathrm{d}\theta^2 + \sin^2\theta\,\mathrm{d}\phi^2 \tag{3}$$

In this metric it is clear that two worldlines, $r = r_0$ and $r = r_1$, are expanding away from each other. There is a cosmological horizon $\mathcal{H}_C$, given by the curve $\Lambda r e^{\Lambda t} = 1$. Integrating the line element along a line of constant t, then $\mathcal{H}_C$ is always at a distance Λ^{-1} away: that is, for $t = t_0$,

$$\int_0^{e^{-\Lambda t_0}/\Lambda} e^{\Lambda t_0}\,\mathrm{d}r = e^{\Lambda t_0}(e^{-\Lambda t_0}/\Lambda - 0) = 1/\Lambda. \tag{4}$$

2.1 Coordinate singularities and the embedded coordinate system

One aspect of the inflationary coordinate system is that it has a coordinate singularity, $\mathcal{H}^\infty$. This coordinate singularity is not explicit as it does not correspond to particular values of the coordinates. This corresponds to the fact that the inflationary coordinate system is not geodesically complete [12]. In order to reach this $\mathcal{H}^\infty$ we need

$$t \to -\infty \quad \text{and} \quad r \to \infty \quad \text{such that} \quad e^{\Lambda t} r \to 1/\Lambda. \tag{5}$$

In order to demonstrate this, we need to introduce a coordinate system which is well-defined around this coordinate singularity, which we define in Section 2.2.

Fortunately there exists a coordinate system which covers the entire de Sitter space without any coordinate singularities. We call this coordinate system the *embedded* coordinate system, $(\xi^1, \xi^2, \xi^3, \xi^4)$ with domain

$$U = \left\{(\xi^1, \xi^2, \xi^3, \xi^4) \in \mathbb{R}^4 \mid \pi/2 < R < 3\pi/2\right\} \tag{6}$$

where

$$R^2 = \sum_{\mu=1}^{4} (\xi^\mu)^2 \tag{7}$$

with the metric given by

$$\mathrm{d}s^2 = \frac{1}{\Lambda^2 R^2 \cos^2(R)} \sum_{\mu=1}^{4} (\mathrm{d}\xi^\mu)^2 - \frac{R^2+1}{\Lambda^2 R^4 \cos^2(R)} \sum_{\mu=1}^{4}\sum_{\nu=1}^{4} \xi^\mu \xi^\nu \, \mathrm{d}\xi^\mu \, \mathrm{d}\xi^\nu \tag{8}$$

The embedded de Sitter space $U \subset \mathbb{R}^4$ is the 4-dimensional ball with a concentric ball hole. It is topologically[1] $\mathbb{R} \times S^3$. The three dimensional version of this ball is depicted in Figure 2.

2.2 Global coordinate system

The relationship between the embedded coordinates and the inflationary coordinates is given via a third coordinate system, called the global coordinate system $(\eta, \rho, \theta, \phi)$

$$-\pi/2 < \eta < \pi/2, \quad 0 < \rho < \pi, \quad 0 < \theta < \pi \quad \text{and} \quad 0 < \phi < 2\pi \tag{9}$$

and conformally flat metric given by

$$\mathrm{d}s^2 = \frac{1}{\Lambda^2 \cos^2(\eta)} (-\mathrm{d}\eta^2 + \mathrm{d}\rho^2 + \sin^2(\rho)\mathrm{d}\omega^2) \tag{10}$$

One problem with the global coordinates is that there are coordinate singularities along the circles '$\rho = 0, \pi$' and '$\theta = 0, \pi$', and we are interested in placing an observer at the point $\rho = 0$.

The coordinate transformation between the inflationary coordinates (t, r, θ, ϕ) and the global coordinates $(\eta, \rho, \theta, \phi)$ is given by

$$e^{\Lambda t} = \tan(\eta) + \sec(\eta)\cos(\rho) \tag{11}$$

$$\Lambda r = \frac{\sin(\rho)}{\sin(\eta) + \cos(\rho)} \tag{12}$$

so that the lines of constant t and r depicted in Figure 1 are given by

$$\eta = \arctan\big(e^{\Lambda t}\big) - \arcsin\big(\cos(\rho)\cos\big(\arctan\big(e^{\Lambda t}\big)\big)\big) \tag{13}$$

$$\rho = \arctan(\Lambda r) + \arcsin(\sin(\eta)\sin(\arctan(\Lambda r))) \tag{14}$$

It may appear that there is something special about the point $(\eta, \rho) = (0, 0)$ at the centre of Figure 1. However, by performing a symmetry action, an $\mathrm{SO}(4,1)$ rotation, we can move any point to the centre of the figure. Except in Section 3.1, we do not need to consider all 4 coordinates of the global coordinate system. Therefore we assume that (η, ρ) corresponds to $(\eta, \rho, \pi/2, 0)$.

We are now in a position to prove (5), how to reach the coordinate singularity $\mathcal{H}^\infty$ in the inflationary coordinate system. We consider a curve, for example $\hat{B}$ given in Figure 3 which tends from $\mathscr{I}^+$ backwards to the point $p_0 = (\rho_0, \eta_0)$ where $\eta_0 = \rho_0 - \pi/2$. At p_0 its tangent vector is X. The coordinates of the curve near p_0 are given by

$$\begin{aligned} \rho &= \rho_0 + \epsilon X^1 \\ \eta &= \eta_0 + \epsilon X^0 \end{aligned} \tag{15}$$

Thus

$$\eta = \rho_0 - \frac{\pi}{2} + \epsilon X^0 \tag{16}$$

Substituting into (11) and (12) gives

$$e^{\Lambda t} = (X^0 - X^1)\epsilon - \frac{1}{2}(X^0 - X^1)^2 \cot(\rho_0)\epsilon^2 + \dots \tag{17}$$

$$\Lambda r = \frac{1}{X^0 - X^1}\epsilon^{-1} - \frac{1}{2}\cot(\rho_0) + \dots \tag{18}$$

which means

$$\Lambda e^{\Lambda t} r = 1 - (X^0 - X^1)\cot(\rho_0)\epsilon + \dots \tag{19}$$

Hence we have to let $t \to -\infty$ and $r \to \infty$ such that $e^{\Lambda t} r = 1/\Lambda$.

[1] We should at this point remark on a topological choice: de Sitter originally considered *not* $\mathbb{R} \times S^3$, but $\mathbb{R} \times \mathbb{R}P^3$ (see [13] and references therein). The metrics are identical, so this is a genuine topological choice. In the latter case, antipodes are identified: this is what allows one to identify the left and right edges of the de Sitter Penrose diagram. This choice is generally ignored or obfuscated in the literature.

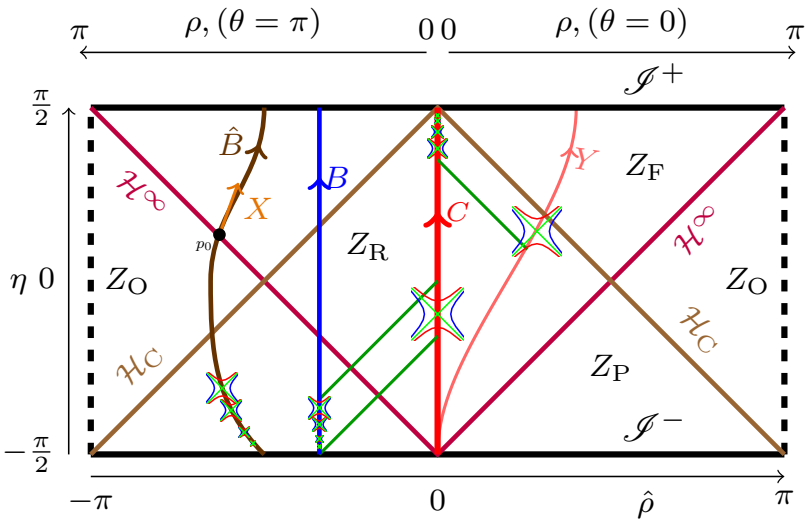

Figure 3. The annulus A, showing both red and blueshift. On the right-hand side, the observer C sees the redshift of the red curve Y as it crosses the horizon $\mathcal{H}_C$. Between the green lightline and $\mathcal{H}_C$, there is only finite proper time for the red curve Y; whereas for the observer C there is infinite proper time. This is depicted in the figure by the number of hyperbolae the worldline crosses.
On the left-hand side, between the two green lightlines, there is infinite proper time for the blue worldline B, but a finite proper time for the observer C. Thus the light from B is infinitely blueshifted.
To avoid infinite blueshift, the dark brown worldline $\hat{B}$, approaches the lightline as it approaches $\mathscr{I}^-$. $\hat{B}$ crosses $\mathcal{H}^\infty$ at p_0, with tangent vector X.

The coordinate transformation between the embedded coordinates $(\xi^1, \xi^2, \xi^3, \xi^4)$ and the global coordinates $(\eta, \rho, \theta, \phi)$ is given by

$$\begin{aligned} \xi^1 &= (\pi + \eta) \sin\rho \, \sin\theta \, \cos\phi, \\ \xi^2 &= (\pi + \eta) \sin\rho \, \sin\theta \, \sin\phi, \\ \xi^3 &= (\pi + \eta) \sin\rho \, \cos\theta \quad \text{and} \\ \xi^4 &= (\pi + \eta) \cos\rho \end{aligned} \tag{20}$$

Substituting (20) into (8) we see that $R = \pi + \eta$.

If we slice de Sitter space by setting $\xi^1 = 0$ and $\xi^2 = 0$, then we obtain the annulus $A = \{(\xi^3, \xi^4) \mid \pi/2 < (\xi^3)^2 + (\xi^4)^2 < 3\pi/2\}$. We can unwrap this annulus by using coordinates $(\eta, \hat{\rho})$ where $-\pi/2 < \eta < \pi/2$, $-\pi < \hat{\rho} < \pi$, and

$$\xi^3 = (\pi + \eta) \sin\hat{\rho} \quad \text{and} \quad \xi^4 = (\pi + \eta) \cos\hat{\rho}. \tag{21}$$

This is depicted in Figure 2. In global coordinates this annulus is a combination of two patches, $\{-\pi/2 < \eta < \pi/2, 0 < \rho < \pi/2, \theta = 0\}$ and $\{-\pi/2 < \eta < \pi/2, 0 < \rho < \pi/2, \theta = \pi\}$, together with the coordinate singularity at $\rho = 0$. This is also depicted in Figure 1.

We can reconstruct M by 'rotating' A in the remaining dimensions. In this case each point in A would correspond to a 2–dimensional hemisphere, with fixed η and ρ. For example, the right-hand side could correspond to the values $\{0 < \theta < \pi/2, 0 < \phi < 2\pi\}$, while the left-hand side, the hemisphere with $\{\pi/2 < \theta < \pi, 0 < \phi < 2\pi\}$. If we take the two points symmetrically about the centre, then together they correspond to the entire 2-sphere[2].

2.3 Partitioning de Sitter space: Copernican worldlines

Let the observer C be the geodesic

$$(\xi^1, \xi^2, \xi^3, \xi^4)|_{C(\zeta)} = \big(0, 0, 0, \pi + \arcsin(\tanh(\Lambda\zeta))\big) \tag{22}$$

where ζ is the worldline parameter (proper time). It is the red vertical line in all the figures. In global coordinates it corresponds to the point $(\eta, \rho)|_{C(\zeta)} = (\arcsin(\tanh(\Lambda\zeta)), 0)$ which is a

[2]We should remark that this how one recovers the 'usual' de Sitter Penrose diagram: by folding the left-hand side of Figure 1 around to the right-hand side, we recover the expected square. We open the diagram up like this to add more detail to the diagram.

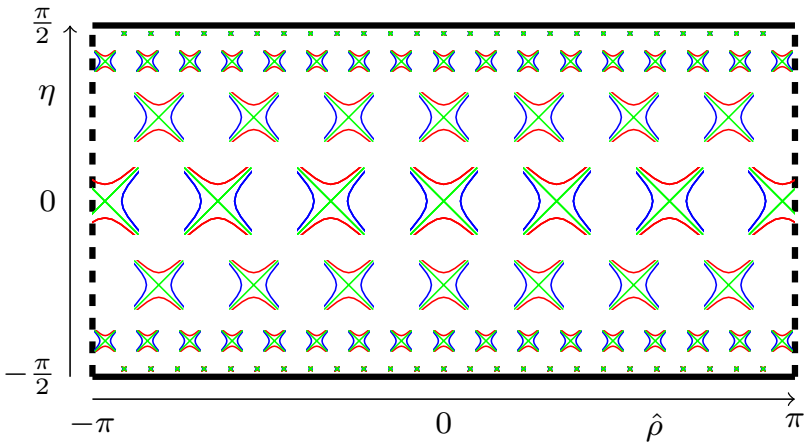

Figure 4. The metric as depicted by the lightcone, together with the unit timelike vectors (red) and unit spacelike vectors (blue) on A. The metric, and therefore the hyperbolae, scale with $\cos(\eta)$.

coordinate singularity. By contrast, on the annulus A, using the $(\eta, \hat{\rho})$ coordinates, it corresponds to $(\eta, \hat{\rho})|_{C(\zeta)} = \big(\arcsin(\tanh(\Lambda\zeta)), 0\big)$ which is not a coordinate singularity. This worldline partitions M into four zones $M = Z_{\mathrm{R}} \cup Z_{\mathrm{F}} \cup Z_{\mathrm{P}} \cup Z_{\mathrm{O}}$ as follows

- Z_{R}. All events which lie in both in the future and past of C, i.e. which are in full causal contact with C. Thus for $q \in Z_{\mathrm{R}}$ the observer can send a signal to q and receive a signal from q and thus establish the radar distance to q. Z_{R} is an open set.
- Z_{F}. All events which lie in the future of C, but not in its past. Thus if $q \in Z_{\mathrm{F}}$, the observer can send a signal to q, but cannot receive a signal from q.
- Z_{P}. All events which lie in the past of C, but not in its future.
- Z_{O}. All events which are not in causal contact with C. This a closed set.

These are depicted in Figure 2 and Figure 3.

The observer C therefore distinguishes two classes of worldlines. The first we will call *initially coincident worldlines* (ICW). These are all worldlines which lie totally inside $Z_{\mathrm{R}} \cup Z_{\mathrm{F}}$. From Figure 1, it is clear that these worldlines must approach $\rho = 0$ as they approach $\mathscr{I}^-$. These include all the red lines in Figure 1. By contrast, we call the set of all worldlines, which are not ICW, *Copernican* worldlines. This reflects the assumption that there is nothing special about ICWs.

Although we call these ICW, they do not have to have an initial zero distance from C. However, there is a maximum distance an ICW can have from C as it approaches $\mathscr{I}^-$. Defining the distance between the observer C and another ICW B as $\Delta(\zeta) = (e^{\Lambda t} r)|_{B(\zeta)}$ then the requirement that B is timelike implies that $\Delta(\zeta) < \Lambda^{-1}$.

The pictorial representation of the metric We can represent the metric on M using the metric hyperboloids, as depicted in Figure 4. These consist of the lightcone, together with timelike (2-sheet) and spacelike (1-sheet) unit hyperboloids. Although these structures actually belong on the tangent space at each point, we can still draw them as though they are on M. These are very useful objects which can be used to give lengths, angles, γ-factors, and many other properties. For a detailed description see [14, 15]. In this article we will use these hyperboloids to depict the red and blueshift.

2.4 The radar coordinate system

The remaining coordinate system is given by the radar coordinates $(\tau, \sigma, \theta, \phi)$ [16]. The advantage of this coordinate system is that one can define a physical distance between a geodesic an event. This is same as in special relativity. One sends a ray out to the event, which reflects the ray back. The time between sending and receiving is divided by two to give the radar distance. This also gives the time coordinate by taking the average of the sending and receiving proper time. Clearly these coordinates are only defined in the region Z_{R}. It is interesting to note that these distances coincide with the spatial geodesic distances given by leaving C along an orthogonal tangent vector. There is a simple observation to establish this result. It is clearly true that the spatial geodesic and

the time slice coincide if the event lies on the horizontal line $\eta = 0$. Likewise the length along C and the length along horizontal line must coincide because the metric is conformal. However there is nothing special about the centre of the diagram, therefore the two coordinate systems must coincide for all points (see Appendix A).

2.5 Reconsidering the inflationary coordinate system

The inflationary coordinates are depicted in Figure 1. They only cover $Z_{\rm R}$ and $Z_{\rm F}$. The boundary between $Z_{\rm R}$ and $Z_{\rm F}$ is the cosmological horizon $\mathcal{H}_{\rm C}$. We can see that all red curves, other than C, will eventually cross $\mathcal{H}_{\rm C}$, and will do so in a finite amount of time. The observer C will never stop being able to see these objects, but their signals will become infinitely redshifted as depicted on the right-hand side of Figure 3. As the object approaches the horizon $\mathcal{H}_{\rm C}$, the angular size of the object remains finite but the radar distance will become infinite.

Once the particle is in $Z_{\rm F}$, one can no longer ascribe a radar distance to the particle. In this case one has to assign a distance according to a preferred coordinate system. It is standard to choose the inflationary coordinate system, and therefore we can make statements such like JADES-GS-z14-1 is 13.9 billion light-years away as we see it, but now it is 46.5 billion light-years away.

In the inflationary coordinate system, the cosmological horizon is at a distance of $1/\Lambda$. That is, if one integrates from C to $\mathcal{H}_{\rm C}$ along a blue line, the result is $1/\Lambda$ (c.f. (4)). By contrast using the global coordinate system the distance to $\mathcal{H}_{\rm C}$ starts off infinite, but tends to $1/\Lambda$ as $\eta \to \pi/2$. More explicitly, in the global coordinate system, the curve specifying $\mathcal{H}_{\rm C}$ is $\eta + \rho = \pi/2$. Thus integrating along a constant $\eta = \eta_0$, we have

$$d_{\mathcal{H}_{\rm C}} = \frac{1}{\Lambda}\int_0^{\pi/2-\eta_0} \frac{{\rm d}\rho}{\cos(\eta_0)} = \frac{1}{\Lambda}\frac{(\pi/2-\eta_0)}{\cos(\eta_0)}. \tag{23}$$

Taking the limit (from above) approaching $\mathscr{I}^-$,

$$\lim_{\eta_0 \to -\pi/2^+} d_{\mathcal{H}_{\rm C}} = \infty \tag{24}$$

and approaching $\mathscr{I}^+$,

$$\lim_{\eta_0 \to \pi/2} d_{\mathcal{H}_{\rm C}} = 1/\Lambda. \tag{25}$$

3 Observations within de Sitter space

3.1 Everything is observed to be rushing towards us!

From Figure 1 and Figure 2 it is clear that the observer C can receive signals from the regions $Z_{\rm R}$ and $Z_{\rm P}$. One can ask what does one observe for objects in $Z_{\rm P}$. Just like events in $Z_{\rm F}$, one cannot assign a radar distance to events in $Z_{\rm P}$. However, unlike $Z_{\rm F}$ there is no preferred coordinate system. Of course there is the contraction coordinate system, where one substitutes $\Lambda \to -\Lambda$ in (3), as well as the global coordinate system. With respect to each of these coordinate systems we can define a notion of distance, either by integrating the line element along lines of constant 'contracting time' (the corresponding time coordinate) for the contracting coordinate system, or lines of constant η for the global coordinate system. With respect to either of these notions of distance, all Copernican worldlines are initially (near $\mathscr{I}^-$) an infinite distance from the observer C. Thus the bulk of what C observes is not everything rushing away from it, but counter intuitively, everything rushing towards it. This even includes light rays which are pointing directly away from it. This is not to say that this light is propagating towards us: rather, the distance described by the coordinate systems above is rapidly decreasing.

An alternative justification for the statement that initially everything is rushing towards us is to consider the observed angular size of distant objects. In the global coordinate system $(\eta, \rho, \theta, \phi)$. Consider the worldline given by $C(\zeta_C) = \big(\arcsin(\tanh(\Lambda\zeta_C)), 0, \pi/2, 0\big)$ where ζ_C is the worldline parameter for C. This observes another object along the worldline $B(\zeta_B) = \big(\eta_B(\zeta_B), \rho_B(\zeta_B), \pi/2, 0\big)$, with ζ_B the worldline parameter of B. The observed object, B has absolute size X_B. We assume that X_B is very small compared to $1/\Lambda$, so that we do not need to worry about the meaning of extended objects in general relativity.

Consider the backward lightcone of the point $C(\zeta_0)$, given by

$$L_{\eta_0}(\hat\eta, \hat\theta, \hat\phi) = \big(\hat\eta, \eta_0 - \hat\eta, \hat\theta, \hat\phi\big) \tag{26}$$

where $\eta_0 = \arcsin(\tanh(\Lambda\zeta_0))$. Then the vector along L_{η_0} at a fixed angle $(\hat{\theta}, \hat{\phi})$ is given by

$$\frac{\partial L_{\eta_0}}{\partial \hat{\eta}} = (1, -1, 0, 0) \tag{27}$$

so that it is clearly lightlike. Solving $L_{\eta_0}(\hat{\eta}, \pi/2, 0) = B(\zeta_B)$, that is, when the backward lightcone intersects B, we see that $\hat{\eta} = \eta_B(\zeta_B) = \eta_0 - \rho_B(\zeta_B)$.

If we consider the angular size of the object at $B(\zeta_B)$ as observed by $C(\zeta_0)$ for fixed $\hat{\theta} = \pi/2$ then the width of the object is between say ϕ_0 and ϕ_1 with $\delta\phi = \phi_1 - \phi_0$. Thus the actual size of the object is

$$X_B = \int_{\phi_0}^{\phi_1} (g(\partial_\phi, \partial_\phi))^{1/2}|_{\rho_B(\zeta_B)}\, \mathrm{d}\hat{\phi} = \frac{\rho_B(\zeta_B)}{\cos(\eta_B(\zeta_B))}\delta\phi \tag{28}$$

hence

$$\delta\phi = X_B\, \frac{\cos(\eta_B(\zeta_B))}{\rho_B(\zeta_B)} \tag{29}$$

Clearly as $\zeta_B \to -\infty$ and $\eta_B(\zeta_B) \to -\pi/2$, then $\delta\phi \to 0$. The same is true for $\delta\theta$. Thus the observation of B by C implies the following: initially C cannot observe B as no signal from B has reached C. We see that C first 'observes' B when

$$\arcsin(\tanh(\Lambda\zeta_C)) = \lim_{\zeta_B \to -\infty} \rho_B(\zeta_B) \tag{30}$$

but with angular size $\delta\phi = 0$. After this the angular size of B increases to a finite size. C could then reasonably conclude that B was rushing towards it. This is independent of the actual trajectory of B, even if it were initially travelling at (near) lightlike velocity away from C. It is even true if B were lightlike, if it had a size and was itself emitting light.

It is natural to ask if it is also blueshifted. Let B be a Copernican worldline with coordinates $B(\zeta_B) = \big(\arcsin(\tanh(\zeta_B)), \rho_0, \pi/2, 0\big)$, where ρ_0 is a constant and ζ_B is the worldline parameter. On the left-hand side of Figure 3, one can see that the finite period on C corresponds to an infinite time the blue worldline B. Thus the light from B is unbounded blushifted.

Mathematically, this is as follows. Consider light travelling from $(\eta_B, \rho_B, \pi/2, 0)$ on B to $(\eta_C, 0, \pi/2, 0)$ on C, as shown in Figure 3. In this case, we are considering a specific B with no peculiar velocity relative to C in the global coordinate system. Thus $\eta_B + \rho_B = \eta_C$. Again, in this specific case, the formula for blueshift is given by

$$\frac{\nu_C}{\nu_B} = \frac{\cos(\eta_C)}{\cos(\eta_B)} \tag{31}$$

which follows from a more general result in Appendix B after imposing B has no peculiar velocity. Thus as $\eta_B \to -\pi/2$ we see that the blueshift becomes infinite. Thus if space was filled with "stars" travelling along lines of constant ρ, then the night sky would be unboundedly blueshifted. We do not have any particular model for the matter in the regions Z_{O} or Z_{P}, thus when we refer to "stars", we mean any light producing source, not necessarily a stellar object.

One can ask what conditions, on the sources, would be necessary to avoid this fate. Let $\hat{B}$ be another path described by a worldline $(\eta, \rho)|_{\hat{B}(\zeta)} = (\eta_{\hat{B}}(\zeta), \rho_{\hat{B}}(\zeta))$ where ζ is the worldline parameter. To normalise $\hat{B}$ we need

$$(\eta'_{\hat{B}})^2 - (\rho'_{\hat{B}})^2 = \cos\big(\eta_{\hat{B}}\big)^2 \tag{32}$$

Let ζ_0 be the time when the light was emitted, and assume $\rho_{\hat{B}}(\zeta_0) > 0$. Then the light will arrive at C at $(\eta, \rho) = (\eta_1, 0) = (\eta_{\hat{B}}(\zeta_0) + \rho_{\hat{B}}(\zeta_0), 0)$. Hence

$$\frac{\nu_C}{\nu_{\hat{B}}} = \frac{\cos(\eta_1)}{(\eta'_{\hat{B}}(\zeta_0) + \rho'_{\hat{B}}(\zeta_0))} \tag{33}$$

Hence to avoid $\nu_C \to \infty$ as $\eta'_{\hat{B}}(\zeta_0) - \rho'_{\hat{B}}(\zeta_0) \to 0$ while $\eta'_{\hat{B}}(\zeta_0) + \rho'_{\hat{B}}(\zeta_0)$ does not tend to zero. In other words $\hat{B}$ must become lightlike as it approaches $\mathscr{I}^-$ (see Figure 3).

We have now seen three results which imply the observers will see everything rushing towards them: the global coordinate system, the angular size of objects and the blueshift.

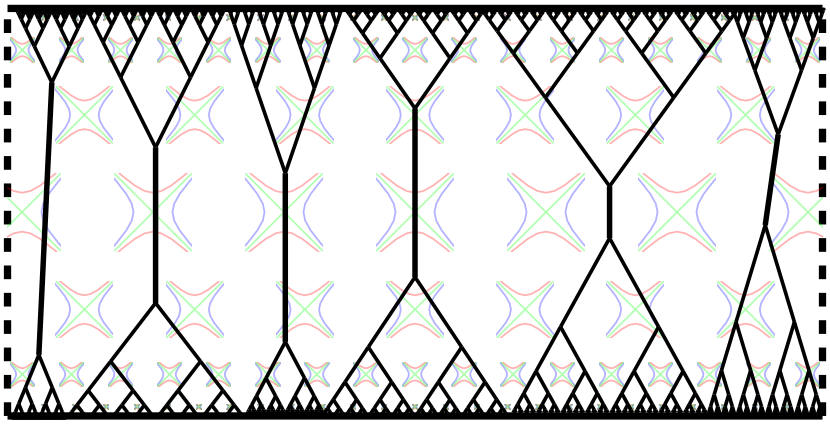

Figure 5. The black lines represent worldlines of particles. As is clear from the figure and the measure (35), the number of particles at $\mathscr{I}^{\pm}$ must be infinite, thus in order to conserve mass, we require the masses to scale as $\cos^3(\eta)$. Since $\mathscr{I}^{-}$ is infinitely dense with particles, all lightlines will end on a particle.

As $\zeta_B \to -\infty$, two effects happen, one the light is more blueshifted, and two the angular size of the object tends to 0. One can ask if the energy of the observed light is finite in the limit.

Suppose $B(\zeta_B)$ is the centre of a ball emitting a constant number of photons per second (in its frame) towards $C(\zeta_C)$. Then even though the angular size of B tends to zero as $\zeta_B \to -\infty$, C still receives all the photons, and in addition, the rate of these photons arriving tends to infinity and so does their frequency. Another way of thinking about this. If C observes B first at the moment, (30), then during the time between ζ_C and $\zeta_C + \delta\zeta$, C receives all the photons emitted by B between $\zeta_B = -\infty$ and $\zeta_B = \delta\zeta\,\Lambda\,\mathrm{sech}(\Lambda\zeta_C)$, which is an infinite amount of proper time.

3.2 Measures and Olbers's paradox

We can now ask the question of how many objects does an observer see. For this we distribute the "stars" randomly according to some measure. There are various ways one can construct a measure on spacelike hypersurfaces of de Sitter space.

Our first measure uses the global coordinate system and is given by

$$\frac{1}{2\pi^2}\sin^2(\rho)\sin(\theta)\,\mathrm{d}\rho\,\mathrm{d}\theta\,\mathrm{d}\phi \tag{34}$$

Using this measure one could choose a spatial hypersurface of constant η and randomly place N "stars". It would then take a finite amount of time for any observer to see any stars. The observation of the stars would then proceed as described in Section 3.1.

An alternative is a coalescing measure. This is given by

$$\frac{1}{2\pi^2\cos^3(\eta)}\sin^2(\rho)\sin(\theta)\,\mathrm{d}\rho\,\mathrm{d}\theta\,\mathrm{d}\phi \tag{35}$$

It is clear that this does not preserve the number of "stars". Thus for this to conserve mass we assume that the masses of the "stars" goes as $\cos^3(\eta)$ and that they coalesce. This is depicted in Figure 5. The result of this that every backward lightline will almost certainly end on a "star". Using this effect, we have something akin to Olbers' paradox, but with infinite blueshift. This is similar to the well-known instability in black hole spacetimes [17, 18].

3.3 Thermalisation

One of the key arguments for inflation is that it enables a small region of spacetime to thermalise before being expanded, and hence why the CMB is such a uniform temperature. However, this is not possible with eternal inflation as two worldlines at $\hat{\rho} = 0$ and $\hat{\rho} = \hat{\rho}_1$ will not have the chance to thermalise until the event $\eta = \hat{\rho}_1$. Indeed, the worldlines at $\hat{\rho} = 0$ and $\hat{\rho} = \pi$ will never be causal contact.

3.4 Maximum number of e-folds of inflation

The simple observation that the night sky does not contain infinitely blueshifted galaxies in every direction implies one of the assumptions of the model presented here is invalid. The current popular model of the universe, ΛCDM, assumes an initial big bang, followed by a period of

inflation. Inflation then stopped and, maybe after some time, a new period of inflation started with a much lower value of Λ. The initial period of inflation has to run for a minimum period, so that our observed universe is flat, over cosmological distances, and is not full of magnetic monopoles. This gives a minimum number of around 50-60 e-folds of initial inflation.

With a reasonable set of assumptions, we can now give an upper bound of the number of e-folds of inflation. Let us assume that there was a finite period of inflation. This started at η_{ini} and stopped at η_{fin}. After that the universe expanded with FLRW metric with conformal scale factor $a(t) = t^{\alpha}$. We need to assume there exist Copernican matter and it is not rushing away from us close to the speed of light. This emits a photon of energy E_{ini} at time η_{ini}. The maximum energy photons we observe today is E_{fin}.

Along C we can calculate the corresponding values of t as $2e^{\Lambda t_{\text{ini}}} = \eta_{\text{ini}} + \pi/2$ and likewise for t_{fin}. To simplify the calculation we assume that both η_{ini} and η_{fin} are close to $-\pi/2$. The number of e-folds of inflation is then given by, using equation (31),

$$2e^{\Lambda(t_{\text{fin}}-t_{\text{ini}})} = \frac{\eta_{\text{fin}} + \frac{\pi}{2}}{\eta_{\text{ini}} + \frac{\pi}{2}} = \frac{\cos(\eta_{\text{fin}})}{\cos(\eta_{\text{ini}})} = \frac{E_{\text{fin}}}{E_{\text{ini}}} = \frac{E_{\text{max}}}{E_{\text{ini}}} \frac{a(t_{\text{now}})}{a(t_{\text{fin}})} = \frac{E_{\text{max}}}{E_{\text{ini}}} \left(\frac{t_{\text{now}}}{t_{\text{fin}}}\right)^{\alpha} \tag{36}$$

since $E_{\text{fin}} = E_{\text{max}} a(t_{\text{now}})/a(t_{\text{fin}})$. To produce an estimate, let us consider the following. Assume $E_{\text{max}} \sim 10^{14}$eV, the approximate order of magnitude above which it is thought the universe is opaque; let $\alpha = 2/3$ such that we are considering dust; and assume that $t_{\text{now}}/t_{\text{fin}} \sim 10^{50}$, which is justified by assuming inflation ended about $\sim 10^{-32}$s after the big bang and assuming that the current age of the universe is $\sim 10^{18}$s. We do have to speculate about E_{ini}: there is no theoretical lower bound for photon energy. The best bound we can give is cosmologically motivated. As previously demonstrated, the 'size' of the universe is $1/\Lambda$, which we can take as a characteristic length scale. Assuming Λ constant, and taking a currently accepted value, we have $E_{\text{ini}} \sim 10^{-33}$eV. These numbers yield a maximum number of e-folds of $\sim \mathcal{O}(10^2)$. This result does not rapidly change as one moves this estimate: changing the order of magnitude of E_{ini} only changes the number of e-folds by $\sim \pm 2$. Thus we would feel confident in saying that, $\mathcal{O}(10^2)$ is a reasonable upper bound for the number of e-folds.

4 Conclusion

We have discussed the theoretical underpinnings of eternal inflation, including its realisation as de Sitter spacetime with various coordinate charts. By adding metric hyperbolae to Penrose diagrams, we gained an understanding of how eternal inflation leads to near infinite blueshift, by the initial contraction phase. Furthermore, we discussed how this relates to Olbers' paradox in the extreme. Briefly, we remarked how in an eternally inflating universe, one should not expect thermalisation, before finally giving a ballpark estimate for the maximum number of e-folds, given certain assumptions in this model.

The fact that we do not observe these ultra-high energy photons, and in-fact we mostly observe redshift, means if we take seriously the idea that our universe did undergo a period of inflation as described then we must resolve why our observations do not match reality. There are a number of obvious explanations we can concoct.

1. The universe has not had past eternal inflation.
2. The universe has been in an eternally inflating phase, but with the condition that...
   (a) there was no Copernican matter.
   (b) there was no Copernican radiation.
   (c) there was Copernican matter, but it was all moving away from us asymptotically close to light speed.
   (d) there was no Copernican matter, but there was Copernican radiation which was all moving away from us.
   (e) all the high energy light was captured by primordial black holes.

This list is not exhaustive: these are those situations which require the least amount of explanation. Clearly though, most explanations require a large breaking of symmetry, and explaining this is not a simple ordeal.

One might think that intervening dust or other matter provides a solution, however this does not appear to be the case. Assuming the distribution of matter is dense enough such that no light from $\mathscr{I}^-$ could reach us directly in order to match observation, then this dust or matter would

glow as bright as the radiation it blocks, so we should still see near-infinite blueshift. Instead, one possible solution could be provided by recombination, since before this time the universe was *essentially* opaque to photons. This would mean the ultra-high energy photons would contribute to warming the universe, possibly extending the plasma phase. It is possible that this would produce detectable effects, and this is a possible direction for future research. In addition, there is also a possibility some of these ultra-high energy photons would pass through $\mathcal{H}^\infty$ and the plasma unaffected.

There are a number of potentially interesting avenues for future research. One can look at different models of the universe, including ones closer to our current understanding of the universe. When considering spherically symmetric models, one can always suppress the spherical dimensions, so as to require only 2-dimensional metrics. Since all such metrics are conformally flat, it is therefore possible to depict the metric on a 2-dimensional diagram such as Figure 4, and the causal structure, Figure 1. One can consider spacetimes which change from a de Sitter metric to another metric, with the boundary given by a hypersurface of constant η. Also, eternal inflation, but where bubble non-inflating universes are formed. In this case, the metric is no longer spherically symmetric, and one can only depict a 2-dimensional slice of spacetime. One can also depict the big rip. In this last case the metric hyperbolae go as $(\eta - \eta_0)^\alpha$ where $0 < \alpha < 1$ and η_0 is the upper limit of η. This enables reaching the end of the universe in finite proper time. One could also investigate models where the intensely blueshifted light is, in fact, the origin of the initial heat of our universe.

Data availability
No new data were created or analysed in this study.

Acknowledgments
The authors would like to thank Drs. David Sloan, Mathew Smith, David Burton, Prof. Konstantinos Dimopoulos and Finlay Gunneberge. SC would like to thank Adam Bac for useful conversations.

Funding
JG would like to thank STFC (ST/V001612/1 The Cockcroft institute). SC would like to thank the EPSRC DTP (EP/W524402/1).

Author contributions
Jonathan Gratus: Conceptualization, both Writing stages. Sam Close: both Writing stages

A Radar Coordinates

Let C be the worldline of our observer, which will follow the line of $\rho = 0$ in our global coordinate system. Then consider some point p: the radar time and distance measured by C to p are given respectively by

$$\tau(p) = \frac{1}{2}(\zeta_2 + \zeta_1) \quad \text{and} \quad \sigma(p) = \frac{1}{2}(\zeta_2 - \zeta_1) \tag{37}$$

where ζ_1 is the time of emission and ζ_2 is the time of reception, as measured by C. Light intercepts C on lines of $\eta \mp \rho$. Since the time experienced along C is a simple integral $\int \sec(\eta)/\Lambda \, \mathrm{d}\eta$, we get the radar time and distance as

$$\tau(p) = \frac{1}{2\Lambda}(f(\eta + \rho) + f(\eta - \rho)) \quad \text{and} \quad \sigma(p) = \frac{1}{2\Lambda}(f(\eta + \rho) - f(\eta - \rho)) \tag{38}$$

where

$$f(x) = \int \sec(x) \, \mathrm{d}x = \ln(\sec(x) + \tan(x)) \tag{39}$$

Using these expressions, we can solve for η, ρ in terms of τ, σ. We also now consider every point that C could measure, hence we drop the evaluation of τ, σ on p. We thus find

$$\tan(\eta) = \frac{e^{\Lambda(\sigma-\tau)}(e^{2\Lambda\tau} - 1)}{e^{2\Lambda\sigma} + 1} \quad \text{and} \quad \tan(\rho) = \frac{e^{\Lambda(\tau-\sigma)}(e^{2\Lambda\sigma} - 1)}{e^{2\Lambda\tau} + 1} \tag{40}$$

After some algebra and some hyperbolic identities, one finds the metric as

$$\mathrm{d}s^2 = \frac{1}{\cosh^2(\Lambda\sigma)} \left(-\mathrm{d}\tau^2 + \mathrm{d}\sigma^2 + \frac{\sinh^2(\Lambda\sigma)}{\Lambda^2}(\mathrm{d}\theta^2 + \sin^2(\theta)\,\mathrm{d}\phi^2) \right) \tag{41}$$

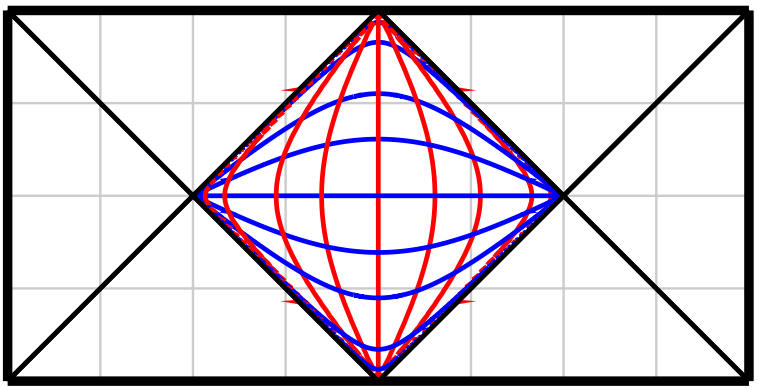

Figure 6. The geodesic and radar coordinate system. The blue curves represent hypersurfaces of constant τ, while the red curves represent worldlines of constant σ.

This coordinate system is depicted on our de Sitter spacetime diagram in Figure 6. An SO(4,1) rotation which preserves C will map the blue curves onto blue curves.

B High Frequency Limit: Calculation of Blueshift

We perform this calculation in the language of differential forms, rather than index notation, as it is the simplest way in this case. For the unfamiliar, see standard textbooks e.g. [19, 20]. To clarify notation, we use angular brackets for the action of a vector field on a scalar field; a colon for the action of a 1-form on a vector; and $\lrcorner$ for the interior product. We denote the metric with g and the inverse metric with $\widetilde{g}$. The rest of the notation is standard. For a treatment of the high-frequency limit, see [21].

Consider the 1-form

$$A = \exp(i\phi/\epsilon)a \tag{42}$$

where a is some complex 1-form describing the amplitude of the wave, ϕ is the phase, and $\epsilon \approx 0$ is an expansion parameter. Then

$$F = \mathrm{d}A = \exp(i\phi/\epsilon)(i\,\mathrm{d}\phi \wedge a/\epsilon + \mathrm{d}a) \tag{43}$$

In the limit $\epsilon \to 0$, the dominating term is

$$F = i\exp(i\phi/\epsilon)\,\mathrm{d}\phi \wedge a/\epsilon \tag{44}$$

The Hodge dual of this is

$$\star F = i\exp(i\phi/\epsilon) \star (\mathrm{d}\phi \wedge a)/\epsilon \tag{45}$$

and the exterior derivative,

$$\mathrm{d} \star F = -\exp(i\phi/\epsilon)\,\mathrm{d}\phi \wedge \star(\mathrm{d}\phi \wedge a)/\epsilon^2 + i\exp(i\phi/\epsilon)\,\mathrm{d}(\star(\mathrm{d}\phi \wedge a))/\epsilon \tag{46}$$

which vanishes by the second vacuum Maxwell equation. We keep the lowest order in ϵ. Thus Maxwell's equation becomes

$$0 = \exp(i\phi/\epsilon)\,\mathrm{d}\phi \wedge \star(\mathrm{d}\phi \wedge a) \tag{47}$$

Using the identities of the Hodge dual,

$$0 = \mathrm{d}\phi \wedge \star(\mathrm{d}\phi \wedge a) = -\star(\mathrm{d}\phi^\sharp \lrcorner (\mathrm{d}\phi \wedge a)) = -\widetilde{g}(\mathrm{d}\phi\,, \mathrm{d}\phi)a + \widetilde{g}(a, \mathrm{d}\phi)\,\mathrm{d}\phi \tag{48}$$

where $\mathrm{d}\phi^\sharp$ is the metric dual of $d\phi$ and $\widetilde{g}$ is the inverse metric. $\mathrm{d}\phi \wedge a \neq 0$, so we must have $\widetilde{g}(\mathrm{d}\phi\,, \mathrm{d}\phi) = 0$ and $\widetilde{g}(a, \mathrm{d}\phi) = 0$; this tells us that the vector $\mathrm{d}\phi^\sharp$ is null, and the amplitude is orthogonal. We should also show that the dual vectors are null *geodesics*. For brevity, let $k := \mathrm{d}\phi^\sharp$. Then consider

$$\nabla_v(g(k,k)) = (\nabla_v g)(k,k) + 2g(\nabla_v k, k) \tag{49}$$

The l.h.s. vanishes since k is null, and the first term on the r.h.s. vanishes by metric compatibility. Then $g(\nabla_v k, k) = 0$. Next, remark that $\mathrm{d}^2\phi = 0$, so

$$\mathrm{d}x^\mu \wedge \nabla_\mu\,\mathrm{d}\phi = 0 \tag{50}$$

Taking the interior product with k,

$$0 = k \lrcorner (\mathrm{d}x^\mu \wedge \nabla_\mu \mathrm{d}\phi) = k^\mu \nabla_\mu \mathrm{d}\phi - ((\nabla_\mu \mathrm{d}\phi) : k)\, \mathrm{d}x^\mu = \nabla_k k \tag{51}$$

Hence k is a null geodesic.

The measured frequency of the wave by an observer C at $p \in M$ is $\nu^C|_p = (\mathrm{d}\phi : \dot{C})|_p = (\dot{C}\langle\phi\rangle)|_p$. Then suppose that B emits a photon at $p \in M$ and C receives this photon at $q \in M$, with $\eta|_q > \eta|_p$ subject to p, q being connected lightlike. Then the ratio of their frequencies

$$\frac{\nu^C|_q}{\nu^B|_p} = \frac{(\dot{C}\langle\phi\rangle)|_q}{(\dot{B}\langle\phi\rangle)|_p} \tag{52}$$

Without loss of generality let $\dot{C} = \Lambda \cos(\eta)\partial_\eta$ so $\dot{C}(\phi) = \Lambda \cos(\eta)\partial_\eta\phi$. We can parameterise a general unit $\dot{B}$ using hyperbolic functions:

$$\dot{B} = \Lambda \cos(\eta)(\cosh(\chi)\partial_\eta + \sinh(\chi)\partial_\rho) \tag{53}$$

where χ is some function of the worldline parameter. It is clear that χ relates to the velocity of the emitter.

Remark that the phase is a function of η, ρ in a specific way: $\phi = \phi_0(\eta + \rho)$. Then this ratio becomes

$$\frac{\nu^C|_q}{\nu^B|_p} = \frac{\cos(\eta|_q)}{\cos(\eta|_p)} e^{-\chi|_p} \tag{54}$$

Firstly, observe that if $\eta|_q = -\eta|_p$, the redshift is determined solely by the peculiar velocity of the source, as specified by χ, which reflects the isometry $\eta \to -\eta$.

The next most obvious question is what happens at late time, i.e. as $q \to \mathscr{I}^+$? Naïvely of course this ratio tends to zero, corresponding to infinite redshift, reflecting the continuous, infinite expansion of space. One can prevent this by choosing $\chi = k + \ln(\cos(\eta))$, which, as one takes the limit $q \to \mathscr{I}^+$, gives a velocity $v_C = 1$: i.e., for the source not to be infinitely redshifted into the distant future, it must be moving towards the observer asymptotically close to lightspeed, as it crosses $\mathcal{H}_C$.

By the aforementioned isometry, this picture is repeated in the converse. That is, if the source is taken to $p \to \mathscr{I}^-$, we can choose $\chi = k + \ln(\sec(\eta))$ to keep the blueshift finite. Similarly, in the limit, this corresponds to the source leaving $\mathscr{I}^-$ at asymptotically lightspeed away from the observer.

By our parameterisation, redshift can only occur if $k < 0$, however, blueshift will always occur.

References

[1] Alan H. Guth. "Inflation and eternal inflation". In: *Physics Reports* 333–334 (Aug. 2000), pp. 555–574. DOI: 10.1016/S0370-1573(00)00037-5. arXiv: astro-ph/0002156 [astro-ph].

[2] Alan H. Guth. "Eternal Inflation". In: *Annals of the New York Academy of Sciences* 950.1 (Jan. 25, 2006), pp. 66–82. DOI: 10.1111/j.1749-6632.2001.tb02128.x. arXiv: astro-ph/0101507 [astro-ph].

[3] Alan H. Guth. "Eternal inflation and its implications". In: *Journal of Physics A: Mathematical and Theoretical* 40.25, 6811 (June 6, 2007). DOI: 10.1088/1751-8113/40/25/S25. arXiv: hep-th/0702178 [hep-th].

[4] Hongbo Cai, Pengjie Zhang, and Yilun Guan. "Eternal inflation bubble collision signature on CMB remote dipole and quadrupole fields". In: *Phys. Rev. D* 113.6, 063545 (Mar. 18, 2026). DOI: 10.1103/4c9h-tk5t. arXiv: 2510.12134 [astro-ph.CO].

[5] Dalila Pîrvu, Jonathan Braden, and Matthew C. Johnson. "Bubble clustering in cosmological first order phase transitions". In: *Phys. Rev. D* 105.4, 043510 (Feb. 8, 2022). DOI: 10.1103/PhysRevD.105.043510. arXiv: 2109.04496 [hep-th].

[6] Raffaele Tito D'Agnolo et al. "A multiverse outside of the swampland". In: *Phys. Rev. D* 110.5, 055007 (Sept. 3, 2024). DOI: 10.1103/PhysRevD.110.055007. arXiv: 2404.13109 [hep-ph].

[7] Stephen W. Hawking and George F. R. Ellis. *The Large Scale Structure of Space-Time*. With a forew. by Abhay Ashtekar. 50th Anniversary Edition. Cambridge Monographs on Mathematical Physics. Cambridge University Press, 2023. DOI: 10.1017/9781009253161.

[8] Arvind Borde, Alan H. Guth, and Alexander Vilenkin. "Inflationary Spacetimes Are Incomplete in Past Directions". In: *Physical Review Letters* 90.15, 151301 (Apr. 15, 2003). DOI: 10.1103/PhysRevLett.90.151301. arXiv: gr-qc/0110012 [gr-qc].

[9] T. Banks and W. Fischler. *An upper bound on the number of e-foldings*. 2004. arXiv: astro-ph/0307459 [astro-ph].

[10] Rong-Gen Cai. "Holography, the cosmological constant and the upper limit of the number of e-foldings". In: *Journal of Cosmology and Astroparticle Physics* 2004.02, 007 (Feb. 14, 2004). DOI: 10.1088/1475-7516/2004/02/007. arXiv: hep-th/0312014 [hep-th].

[11] Daniel Phillips, Andrew Scacco, and Andreas Albrecht. "Holographic bounds and finite inflation". In: *Physical Review D: Particles and Fields* 91.4, 043513 (Feb. 11, 2015). DOI: 10.1103/PhysRevD.91.043513. arXiv: 1410.6065 [gr-qc].

[12] Daisuke Yoshida and Jerome Quintin. "Maximal extensions and singularities in inflationary spacetimes". In: *Classical and Quantum Gravity* 35.15, 155019 (July 16, 2018). DOI: 10.1088/1361-6382/aacf4b. arXiv: 1803.07085 [gr-qc].

[13] Brett McInnes. "De Sitter and Schwarzschild-de Sitter according to Schwarzschild and de Sitter". In: *Journal of High Energy Physics* 2003.09, 009 (Sept. 19, 2003). DOI: 10.1088/1126-6708/2003/09/009. arXiv: hep-th/0308022 [hep-th].

[14] Jonathan Gratus. *A pictorial introduction to differential geometry, leading to Maxwell's equations as three pictures*. 2017. arXiv: 1709.08492 [math.DG].

[15] William L. Burke. *Spacetime, Geometry, Cosmology*. Ed. by Donald E. Osterbrock and Joseph S. Miller. University Science Books, 1980.

[16] Volker Perlick. "On the Radar Method in General-Relativistic Spacetimes". In: *Lasers, Clocks and Drag-Free Control. Exploration of Relativistic Gravity in Space*. Ed. by Hansjörg Dittus, Claus Lämmerzahl, and Slava G. Turyshev. Vol. 349. Astrophysics and Space Science Library. Springer, 2008, pp. 131–152. DOI: 10.1007/978-3-540-34377-6_5. arXiv: 0708.0170 [gr-qc].

[17] Michael Simpson and Roger Penrose. "Internal Instability in a Reissner-Nordström Black Hole". In: *International Journal of Theoretical Physics* 7.3 (Apr. 1973), pp. 183–197. DOI: 10.1007/BF00792069.

[18] Subrahmanyan Chandrasekhar and J. B. Hartle. "On crossing the Cauchy horizon of a Reissner–Nordström black-hole". In: *Proceedings of the Royal Society of London. A. Mathematical and Physical Sciences* 384.1787 (Dec. 1982), pp. 301–315. DOI: 10.1098/rspa.1982.0160.

[19] Tevian Dray. *Differential Forms and the Geometry of General Relativity*. CRC Press LLC, 2014. DOI: 10.1201/b17620.

[20] Paul Renteln. *Manifolds, Tensors, and Forms. An Introduction for Mathematicians and Physicists*. Cambridge University Press, 2013. DOI: 10.1017/CBO9781107324893.

[21] Volker Perlick. *Ray Optics, Fermat's Principle, and Applications to General Relativity*. Lecture Notes in Physics Monographs. Springer, 2000. DOI: 10.1007/3-540-46662-2.